



Theoretical investigation of the sound attenuation of membrane-type acoustic metamaterials

Yuguang Zhang ^{a,b}, Jihong Wen ^{a,b}, Yong Xiao ^{a,b}, Xisen Wen ^{a,b,*}, Jianwei Wang ^{a,b}

^a MOE Key Laboratory of Photonic and Phononic Crystals, and Institute of Mechatronical Engineering, National University of Defense Technology, Changsha, Hunan 410073, PR China

^b Laboratory of Science and Technology on Integrated Logistics Support, National University of Defense Technology, Changsha, Hunan 410073, PR China

ARTICLE INFO

Article history:

Received 18 December 2011

Received in revised form 4 March 2012

Accepted 5 March 2012

Available online 9 March 2012

Communicated by R. Wu

Keywords:

Acoustic metamaterials

Membrane

Sound attenuation

Transmission loss

ABSTRACT

Membrane-type acoustic metamaterials have been recently shown to exhibit good performance of sound attenuation in a low frequency range. An analytical approach for the fast calculation of sound transmission loss of the membrane-type acoustic metamaterials is presented here. The discussion indicate that the first transmission loss valley and the transmission loss peak depend strongly on the attaching mass, while the second transmission loss valley is mainly influenced by the membrane properties. The effects of membrane tension and mass position on the transmission loss and characteristic frequencies are also discussed in detail.

© 2012 Elsevier B.V. All rights reserved.

1. Introduction

Acoustic barriers with effective sound insulation performance can find many useful applications in the area of aerospace, automotive vehicles and environmental noise control. However, traditional acoustic barriers are always not effective at low frequencies due to the mass law. Recently, the emergence of acoustic metamaterials provides new ideas to this problem [1–13]. Extensive efforts are being exerted to develop various types of acoustic metamaterials to achieve low frequency sound attenuation. Of particular interest is a thin, lightweight membrane-type acoustic metamaterials which has been shown to exhibit unique sound insulating performance. The transmission loss (TL) of this type of acoustic metamaterials has a significant increase over mass law predictions for a narrow band at low frequencies [10–13]. The pioneering work of Yang et al. has demonstrated experimentally and theoretically that a circular elastic membrane with a small circular weight attached to the center can operate sound transmission effectively in the 100–1000 Hz frequency range [10]. In their latter work, they have further shown experimentally that a square membrane carrying a small circular weight can insulate sound over a broad frequency range from 50 to 1000 Hz [11]. More recently,

Naify et al. have examined the influence of mass magnitude and membrane tension on the TL by experimental measurements and finite element analysis (FEA), and mapped the dynamic response of the structure under acoustic loading using a laser vibrometer [12]. In their continuous work, the TL behavior of multiple elements arranged in arrays has been measured experimentally, and the effect of the frames structure compliance has been evaluated [13].

The membrane-type acoustic metamaterials can be described as an elastic membrane carrying a concentrated mass. The vibration eigenfrequencies can be tuned by varying the membrane and mass properties. Many publications on the free vibrations of plate carrying a concentrated/distributed mass have been presented, but there is an essential difference between the vibration of a membrane and of a thin plate. In a membrane, the restoring force arises entirely from the tension applied to the membrane, whereas in a thin plate the restoring force results from the stiffness of the diaphragm. Moreover, the effects of air should be properly considered, for the lightweight membrane structures vibrating in air have lower natural frequencies and higher damping than in vacuum. FEA (COMSOL Multiphysics) has been used to calculate the TL of the membrane-mass structure [8,10,11]. However, large time and computational costs are required in the preprocessing, solution and postprocessing of a given design. In practice, especially in the initial design stage, a fast and accurate assessment of the performance of the membrane-type acoustic metamaterials is of great interest.

* Corresponding author at: MOE Key Laboratory of Photonic and Phononic Crystals, and Institute of Mechatronical Engineering, National University of Defense Technology, Changsha, Hunan 410073, PR China. Tel./fax: +86 731 8457 4975.

E-mail address: wenxs@vip.sina.com (X. Wen).



膜型声学超材料声衰减的理论研究

张玉光, 文继红, 肖勇, 文喜森, 王建伟

^a 国防科技大学光子和声子晶体 MOE 重点实验室, 机电工程学院, 中国湖南省长沙市 410073
^b 国防科技大学综合后勤保障科学技术实验室, 中国湖南省长沙市 410073

一篇文章

in fo

摘要

文章历史:

收到日期: 2011 年 12 月 18 日 修订稿收到日期:
2012 年 3 月 4 日 接受日期: 2012 年 3 月 5 日
在线发布日期: 2012 年 3 月 9 日 通讯作者: 吴
R.

膜型声学超材料最近表现出在低频范围内具有良好的声音衰减性能。本文提出了一种用于快速计算膜型声学超材料声传输损失的分析方法。讨论表明, 第一个传输损失谷和传输损失峰强烈依赖于附加质量, 而第二个传输损失谷主要受膜性能影响。膜张力和质量位置对传输损失和特征频率的影响也进行了详细讨论。

关键词:

声学超材料 薄膜 声衰减 传输
损失

© 2012 Elsevier B.V. 版权所有。保留所有权利。

1. 介绍 具有有效隔音性能的声学屏障可以在航空航天、汽车车辆和环境噪音控制领域找到许多有用的应用。然而, 传统的声学屏障在低频时通常不够有效, 这是由于质量定律。最近, 声学超材料的出现为这一问题提供了新的思路。正在付出大量努力开发各种类型的声学超材料, 以实现低频声音衰减。特别感兴趣的是, 一种薄、轻质膜型声学超材料, 已被证明具有独特的隔音性能。这种声学超材料的传输损耗 (TL) 在低频窄带上显著增加, 超过了质量定律对低频的预测。杨等人的开创性工作实验证明, 一个带有小圆形重物附在中心的圆形弹性膜可以有效地在 100–1000 赫兹频率范围内传输声音。在他们的后期工作中, 他们进一步通过实验证明, 一个携带小圆形重物的正方形膜可以在从 50 到 1000 赫兹的广泛频率范围内隔音。更近期,

Naify 等人通过实验测量和有限元分析 (FEA) 研究了质量大小和膜张力对 TL 的影响, 并利用激光振动计映射了结构在声载荷下的动态响应 [12]。在他们的持续工作中, 已经通过实验测量了排列成阵列的多个元素的 TL 行为, 并评估了框架结构的顺应性效应 [13]。

膜型声学超材料可以描述为携带集中质量的弹性膜。通过改变膜和质量特性可以调节振动固有频率。关于携带集中/分布质量的板的自由振动已经有很多出版物, 但是膜和薄板的振动之间存在本质区别。在膜中, 恢复力完全来自施加在膜上的张力, 而在薄板中, 恢复力来自隔膜的刚度。此外, 应该适当考虑空气的影响, 因为在空气中振动的轻质膜结构比在真空中具有更低的固有频率和更高的阻尼。FEA (COMSOL Multiphysics) 已被用于计算膜-质量结构的 TL [8, 10, 11]。然而, 在给定设计的预处理、解决方案和后处理中需要大量的时间和计算成本。在实践中, 特别是在初始设计阶段, 对膜型声学超材料性能的快速准确评估具有极大的兴趣。

*通讯作者: 国防科技大学光子和声子晶体教育部重点实验室、机电工程学院, 湖南长沙 410073, 中华人民共和国。电话/传真: +86 731 8457 4975。

电子邮件地址: wenxs@vip.sina.com (X. Wen)。

In this Letter, we present an analytical approach to predict the TL of membrane-type acoustic metamaterials. The validity of the model and method presented in this Letter is confirmed by comparing our analytical results with the FEA calculations reported by Naify et al. The eigenmodes of the acoustic metamaterials are theoretically and numerically analyzed to demonstrate that the first resonance and TL peak frequencies depend strongly on the attaching mass, while the second resonance frequency is mainly influenced by the property of membrane. Furthermore, the effects of the parameters of the mass and membrane on characteristic frequencies are studied in detailed.

2. Analytical model and formulation

The basic unit of the membrane-type acoustic metamaterials can be described as an elastic membrane carrying a small mass, the rim of the membrane was fixed. Consider a cell of membrane-type acoustic metamaterials in an x, y coordinate system. It is subject to biaxial tension T per unit length, which will be assumed to remain constant when the membrane vibrates. The width, length, density per unit area of the membrane are L_x, L_y, ρ_s , and the width, length, density per unit area of the mass are l_x, l_y, ρ_{mass} . The point (x_0, y_0) represents the corner of the mass which is closest to the origin. In Cartesian coordinates, $w(x, y, t)$ represents the transverse displacement in z direction of a point (x, y) at time t . If we treat the inertia forces of the mass as externally concentrated force [14–17], the differential equation of motion of a membrane-mass system in vacuum is given by

$$\rho_s \frac{\partial^2 w}{\partial t^2} + \rho_{mass} \hbar(x, y, x_0, y_0, l_x, l_y) \frac{\partial^2 w}{\partial t^2} - T \nabla^2 w = 0. \quad (1)$$

Here two significant assumptions are that the bending stiffness of the membrane is ignored and the mass does not prevent the bending of the membrane segment on which it is [15]. $\hbar(x, y, x_0, y_0, l_x, l_y)$ represents a combination of four Heaviside functions as follows

$$\begin{aligned} \hbar(x, y, x_0, y_0, l_x, l_y) = & [H(x - x_0) - H(x - x_0 - l_x)] \\ & \cdot [H(x - y_0) - H(x - y_0 - l_y)]. \end{aligned} \quad (2)$$

Now consider that a plane sound wave of frequency ω is normally impinged upon the membrane from the region $z < 0$. The pressure on the membrane-air interface is linked by the normal particle velocity of the membrane which moves with a normal velocity equal to the velocity of the membrane [18]. Hence, the equation of motion including the acoustic loading can therefore be written as

$$\begin{aligned} \rho_s \frac{\partial^2 w}{\partial t^2} + \rho_{mass} \hbar(x, y, x_0, y_0, l_x, l_y) \frac{\partial^2 w}{\partial t^2} \\ + 2\rho_1 c_1 \frac{\partial w}{\partial t} - T \nabla^2 w = 2\tilde{A}e^{j\omega t}, \end{aligned} \quad (3)$$

where \tilde{A} denotes the amplitude of the incident pressure.

Using the mode superposition theory [15,16], $w(x, y, t)$ can be written as a superposition of the mode functions $W_n(x, y)$ multiplying the corresponding time-dependent, generalized co-ordinate $q_n(t)$, i.e.,

$$w(x, y, t) = \sum_{n=1}^N W_n(x, y) q_n(t). \quad (4)$$

The mode function of the membrane with fixed rim can be written as

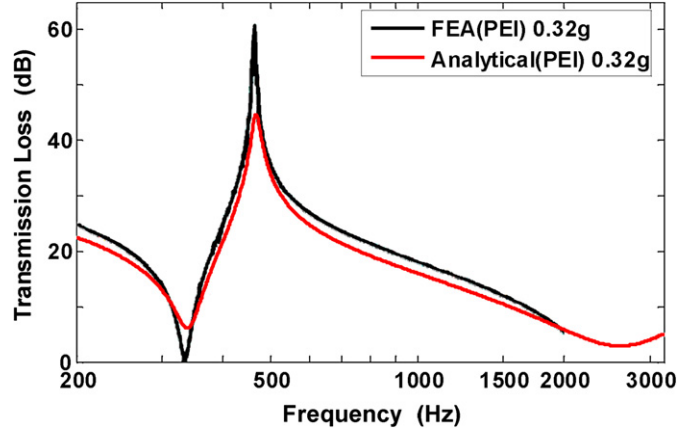


Fig. 1. Analytically predicted transmission loss compared with the FEA calculation measurement by Naify et al. [13].

$$W_n(x, y) = \sin \frac{r\pi}{L_x} x \sin \frac{s\pi}{L_y} y, \quad r = 1, 2, \dots, N_x; s = 1, 2, \dots, N_y; n = N_y(r-1) + s. \quad (5)$$

The membrane performing harmonic vibration under the harmonic acoustic excited, the generalized co-ordinate $q_m(t)$ has the form

$$q_n(t) = \tilde{q}_n e^{j\omega t}. \quad (6)$$

Substituting Eqs. (4), (6) into Eq. (3), multiplying each term by $W_m(x, y)$ and integrating all terms over the domain ($0 \leq x \leq L_x$, $0 \leq y \leq L_y$), we obtain the following equation

$$-\omega^2 M_m \tilde{q}_m - \omega^2 \rho_{mass} \sum_{n=1}^N I_{m,n} \tilde{q}_n + j\omega C_m \tilde{q}_m + K_m \tilde{q}_m = 2\tilde{A} H_m, \quad m = 1, 2, \dots, N \quad (7)$$

where

$$\begin{aligned} M_m &= \rho_s \int_0^{L_x} \int_0^{L_y} W_m \sum_{n=1}^N W_n dx dy, \\ I_{m,n} &= \int_{x_0}^{x_0+l_x} \int_{y_0}^{y_0+l_y} W_m W_n dx dy, \\ C_m &= 2\rho_1 c_1 \int_0^{L_x} \int_0^{L_y} W_m \sum_{n=1}^N W_n dx dy, \\ K_m &= - \int_0^{L_x} \int_0^{L_y} W_m T \nabla^2 \sum_{n=1}^N W_n dx dy, \\ H_m &= \int_0^{L_x} \int_0^{L_y} W_m dx dy. \end{aligned}$$

Eq. (7) can be written as the following matrix form

$$-\omega^2 \{[\mathbf{M}] + [\mathbf{Q}]\} \{\tilde{\mathbf{q}}\} + j\omega [\mathbf{C}] \{\tilde{\mathbf{q}}\} + [\mathbf{K}] \{\tilde{\mathbf{q}}\} = 2\tilde{A} \{\mathbf{H}\} \quad (8)$$

where

$$[\mathbf{M}] = \begin{bmatrix} M_1 & & & & 0 \\ & M_2 & & & \\ & & \ddots & & \\ & & & M_N & \end{bmatrix}, \quad [\mathbf{C}] = \begin{bmatrix} C_1 & & & & 0 \\ & C_2 & & & \\ & & \ddots & & \\ & & & 0 & C_N \end{bmatrix},$$

在这封信中，我们提出了一种分析方法来预测膜型声学超材料的透射损耗。通过将我们的分析结果与 Naify 等人报告的有限元分析计算进行比较，验证了本信中提出的模型和方法的有效性。声学超材料的特征模态在理论上和数值上进行了分析，以证明第一共振和透射损耗峰频率强烈依赖于附加质量，而第二共振频率主要受膜的性质影响。此外，详细研究了质量和膜的参数对特征频率的影响。

2. 分析模型和公式 膜型声学超材料的基本单元可以描述为携带小质量的弹性膜，膜的边缘被固定。考虑一个膜型声学超材料的单元在 x 、 y 坐标系中。它受到单位长度的双轴张力 T 的作用，当膜振动时将假定保持恒定。膜的宽度、长度、单位面积密度分别为 L 、 L 、 ρ ，质量的宽度、长度、单位面积密度分别为 1 、 1 、 ρ 。点 (x, y) 表示质量的角落，最靠近原点。在笛卡尔坐标系中， $w(x, y, t)$ 表示时间 t 时点 (x, y) 在 z 方向的横向位移。如果我们将质量的惯性力视为外部集中力[14–17]，则真空中膜质量系统的运动微分方程为

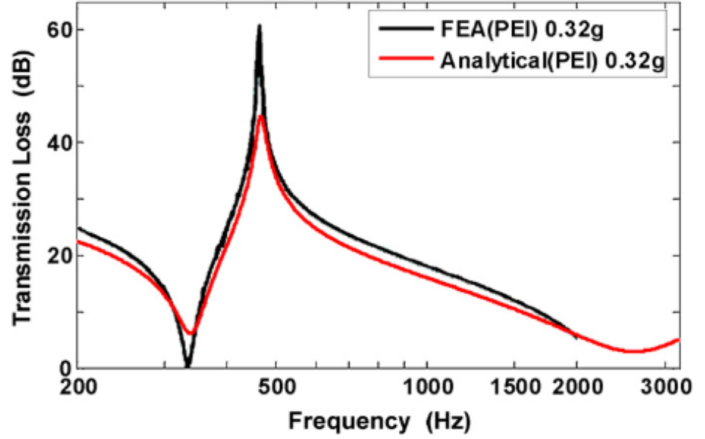


图 1. 分析预测的传输损失与 Naify 等人的有限元分析测量结果进行比较。

$$W(x, y) = \sin \frac{r\pi}{L} x \sin \frac{s\pi}{L} y,$$

$$r = 1, 2, \dots, N; s = 1, 2, \dots, N; n = N(r \oplus 1) + s$$

在谐波激励下执行谐波振动的膜，广义坐标 $q(t)$ 的形式

$$q(t) = \tilde{q} e^{i\omega t}. \quad (6)$$

将方程(4)，(6)代入方程(3)，将每一项乘以 $W(x, y)$ 并将所有项在域 $(0 \leq x \leq L, 0 \leq y \leq L)$ 上积分，我们得到以下方程。

$$-\omega M \tilde{q} - \omega \rho \sum_{n=1}^N \tilde{q}_n j \omega C \tilde{q}_n + K \tilde{q} = 2 \tilde{A} H, \quad m = 1, 2, \dots, N \quad (7)$$

其中

$$M = \rho \int_0^L \int_0^L W dx dy, \quad \sum_{n=1}^N$$

$$I = \int_0^L \int_0^L W W dx dy,$$

$$C = 2 \rho c \int_0^L \int_0^L W dx dy, \quad \sum_{n=1}^N$$

$$K = - \int_0^L \int_0^L W T \nabla W dx dy, \quad \sum_{n=1}^N$$

$$H = \int_0^L \int_0^L W dx dy.$$

方程(7)可以写成以下矩阵形式

$$\{-\omega [M] + [Q]\} \{\tilde{q}\} + j\omega [C]\{\tilde{q}\} + [K]\{\tilde{q}\} = 2 \tilde{A} H \quad (8)$$

其中

$$[M] = \begin{bmatrix} M & & & & \\ & M & & & \\ & & \ddots & & \\ & & & M & \\ & & & & M \end{bmatrix}, \quad [C] = \begin{bmatrix} C & & & & \\ & C & & & \\ & & \ddots & & \\ & & & C & \\ & & & & C \end{bmatrix},$$

$$\rho \frac{\partial^2 w}{\partial t^2} + \rho h(x, y, x, y, 1, 1) \frac{\partial^2 w}{\partial t^2} - T \nabla w = 0. \quad (1)$$

这里有两个重要的假设，即忽略膜的弯曲刚度和质量不会阻止膜段的弯曲[15]。
 $h(x, y, x, y, 1, 1)$ 表示四个 Heaviside 函数的组合如下

$$h(x, y, x, y, 1, 1) = [H(x-x) - H(x-x-l)] [H(y-y) - H(y-y-l)], \quad (2)$$

现在考虑一个频率为 ω 的平面声波正常地作用在膜上，从区域 $z < 0$ 。膜-空气界面上的压力与膜的法线粒子速度相关，该速度与膜的速度相等[18]。因此，包括声学载荷的运动方程可以写成：

$$\rho \frac{\partial^2 w}{\partial t^2} + \rho h(x, y, x, y, 1, 1) \frac{\partial^2 w}{\partial t^2} + 2\rho c \frac{\partial w}{\partial t} - T \nabla w = 2 \tilde{A} e, \quad (3)$$

其中 \tilde{A} 表示入射压力的幅度。

使用模态叠加理论[15, 16]， $w(x, y, t)$ 可以写成模态函数 $W(x, y)$ 乘以相应的时间相关的广义坐标 $q(t)$ 的叠加形式，即，

$$w(x, y, t) = \sum_{n=1}^N W(x, y) q_n(t). \quad (4)$$

膜的模式函数可以写成固定边缘

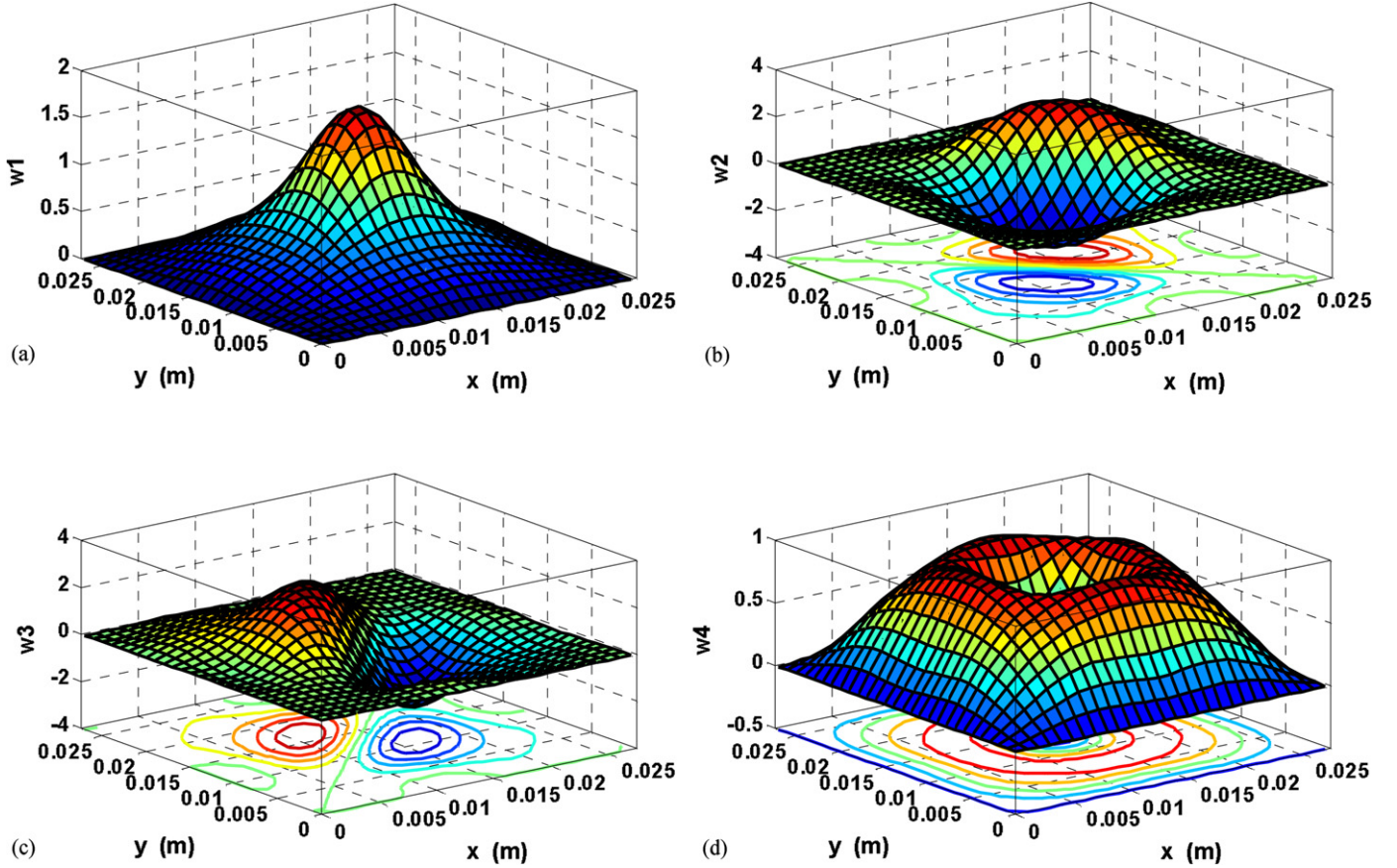


Fig. 2. The first four mode shapes of the membrane unit (without load), (a) first mode, (b) second mode, (c) third mode, (d) fourth mode.

$$\begin{aligned} [\mathbf{K}] &= \begin{bmatrix} K_1 & 0 \\ K_2 & \ddots \\ 0 & K_N \end{bmatrix}, \\ \{\mathbf{H}\} &= \begin{bmatrix} H_1 \\ H_2 \\ \vdots \\ H_N \end{bmatrix}, \quad \{\mathbf{W}\} = \begin{bmatrix} W_1 \\ W_2 \\ \vdots \\ W_N \end{bmatrix}, \quad \{\tilde{\mathbf{q}}\} = \begin{bmatrix} \tilde{q}_1 \\ \tilde{q}_2 \\ \vdots \\ \tilde{q}_N \end{bmatrix}, \\ [\mathbf{Q}] &= \rho_{mass} \begin{bmatrix} I_{1,1} & I_{1,2} & \cdots & I_{1,N} \\ I_{2,1} & I_{2,2} & \cdots & I_{2,N} \\ \vdots & \vdots & \ddots & \vdots \\ I_{N,1} & I_{N,2} & \cdots & I_{N,N} \end{bmatrix}. \end{aligned}$$

From Eq. (8), we have

$$\{\tilde{\mathbf{q}}\} = \frac{\tilde{A}}{-\omega^2\{[\mathbf{M}] + [\mathbf{Q}]\} + j\omega[\mathbf{C}] + [\mathbf{K}]}\{\mathbf{H}\}. \quad (9)$$

The displacement amplitude $\tilde{w}(x, y)$ can be derived from Eqs. (4) and (6), given by

$$\tilde{w}(x, y) = \sum_{n=1}^N W_n(x, y)\tilde{q}_n = \{\mathbf{W}\}^T \{\tilde{\mathbf{q}}\}. \quad (10)$$

Then we can get the analytical expression of the sound amplitude transmission coefficient [18]

$$t_p = \left| \frac{j2\rho_1 c_1 \omega}{L_x L_y} \{\mathbf{H}\}^T \frac{1}{-\omega^2\{[\mathbf{M}] + [\mathbf{Q}]\} + j\omega[\mathbf{C}] + [\mathbf{K}]} \{\mathbf{H}\} \right|. \quad (11)$$

The transmission loss (TL) can be written as

$$TL = 20 \log_{10}(1/t_p). \quad (12)$$

3. Validation of the method

In theory, Eq. (4) is correct only if the mode number N approaches infinity but, in practice, Eq. (4) will give satisfactory results by taking the mode number larger than 9. A significant assumption in the analytical model is that the mass does not prevent the bending of the membrane segment on which it is, so internal resonant of this membrane segment will occur when N is larger than a certain value. But in fact, this membrane segment is difficult to bend for the stiffness of the mass. In order to avoid the internal resonant of this membrane segment, the N shouldn't be set too large.

To verify the validity of the analytical approach developed in the above section, the results obtained here will be compared with the FEA calculations. In Eq. (7), we integrate the I over the surface of the mass. Therefore, we keep the surface area of mass the same as the publication in our calculation. Fig. 1 shows the analytical prediction of TL compared with the FEA results of Naify et al. [13]. The given data are: $T = 486.4$ N/m (PEI), $\rho_s = 0.0912$ kg/m², $L_x = L_y = 27.4$ mm, $m = 0.32$ g (mass magnitude), $r = 1.93$ mm (mass radius). In our calculation, the data are chosen as: $l_x = l_y = (\pi r^2)^{1/2}$, $\rho_{mass} = m/(l_x \times l_y)$ kg/m². The comparison indicates that the present analytical method closely agree with the solution from the reference.

4. Discussions

The remarkable features in Fig. 1 are the two valleys at 338 and 2605 Hz, respectively, and one peak at 467 Hz. In order to investigate the reasons of these characteristic frequencies, the eigenmode of the membrane unit (without load) was studied. From Eq. (1),

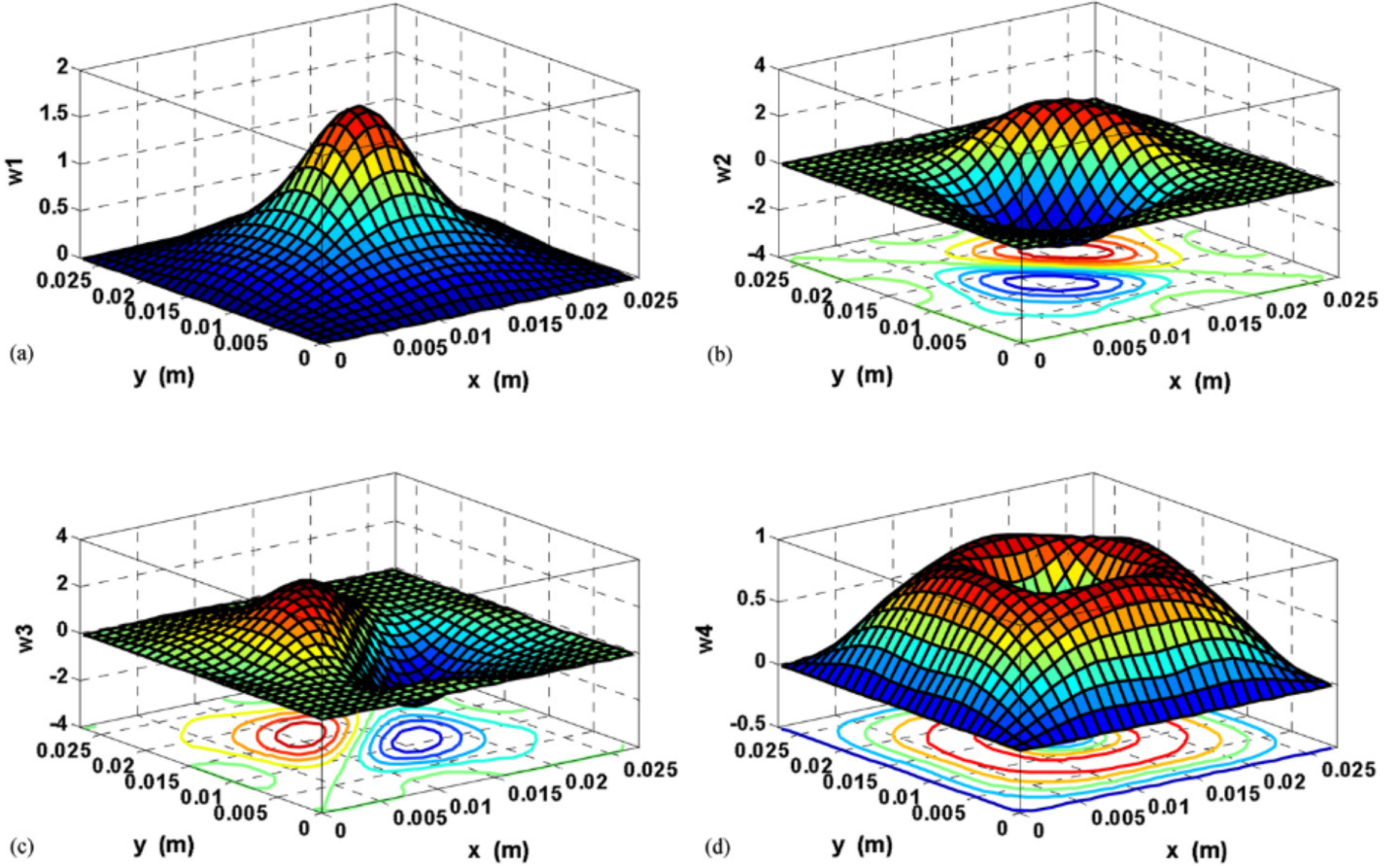


图 2. 薄膜单元的前四种模态形状(无载荷), (a) 第一模态, (b) 第二模态, (c) 第三模态, (d) 第四模态。

$$[K] = \begin{bmatrix} K & & & 0 \\ & K & & \\ & & \ddots & \\ & & & K \end{bmatrix},$$

$$\{H\} = \begin{bmatrix} 0 \\ H \\ H \\ \vdots \end{bmatrix}, \quad \{W\} = \begin{bmatrix} K \\ W \\ W \\ \vdots \end{bmatrix}, \quad \{\tilde{q}\} = \begin{bmatrix} \tilde{q} \\ \tilde{q} \\ \vdots \end{bmatrix},$$

$$[Q] = \rho \begin{bmatrix} H & W & & & & \\ \text{我 我} & \cdot \cdot \cdot & \text{我} & & & \\ \text{我 我} & \cdot \cdot \cdot & \text{我} & & & \\ \vdots & \vdots & \ddots & \ddots & & \\ & & & & \ddots & \\ I & I & \cdots & I & & \end{bmatrix}.$$

从方程(8)中, 我们有

$$\{\tilde{q}\} = \frac{-\omega\{[M] + [Q]\} + j\omega[C] + [K]}{-\omega\{[M] + [Q]\} + j\omega[C] + [K]} \{H\}. \quad (9)$$

位移幅度 $\tilde{w}(x, y)$ 可以从方程(4)和(6)推导得出, 如下所示

$$\tilde{w}(x, y) = \sum_{n=1}^N w(x, y) \tilde{q}_n = \{W\} \{\tilde{q}\}. \quad (10)$$

然后我们可以得到声音幅度传输系数的解析表达式[18]

$$t = \left| \frac{j2\rho c\omega}{L L} \{H\} \frac{1}{-\omega\{[M] + [Q]\} + j\omega[C] + [K]} \{H\} \right|. \quad (11)$$

传输损耗 (TL) 可以写成

$$TL = 20 \log(1/t). \quad (12)$$

3. 方法的验证从理论上讲, 当模式数 N 趋近于无穷大时, 方程(4)才是正确的, 但在实践中, 通过取大于 9 的模式数, 方程(4)将给出令人满意的結果。在分析模型中的一个重要假设是质量不会阻止膜片段的弯曲, 因此当 N 大于某个值时, 这个膜片段的内部谐振会发生。但实际上, 由于质量的刚度, 这个膜片段很难弯曲。为了避免这个膜片段的内部谐振, N 不应设置得太大。

为了验证上述部分开发的分析方法的有效性, 这里得到的结果将与有限元分析计算进行比较。在方程(7)中, 我们对质量表面上的 I 进行积分。因此, 在我们的计算中, 我们保持质量的表面积与出版物中的相同。图 1 显示了与 Naify 等人的有限元分析结果相比, TL 的分析预测。给定数据为: $T = 486.4$ N/m (PEI), $\rho = 0.0912$ kg/m, $L = L = 27.4$ mm, $m = 0.32$ g (质量大小), $r = 1.93$ mm (质量半径)。在我们的计算中, 数据选择为: $l = l = (\pi r)$, $\rho = /(\times)/$ 。比较表明, 目前的分析方法与参考文献中的解决方案非常一致。

4. 讨论 图 1 中显著的特征是分别在 338 和 2605 赫兹处的两个谷和 467 赫兹处的一个峰。为了研究这些特征频率的原因, 研究了膜单元(无负载)的特征模态。从方程(1)中,

we can get the eigenvalue equation of the membrane-type acoustic metamaterials

$$\{\omega^2 \{[\mathbf{M}] + [\mathbf{Q}]\} - [\mathbf{K}]\} \{\tilde{\mathbf{q}}\} = 0. \quad (13)$$

The eigenvalue $\bar{\omega}_j$ and the eigenvector $\{\tilde{\mathbf{q}}\}^j$ ($j = 1, \dots, N$) can be obtained using the Jacobi method. The corresponding natural mode shape $\bar{w}_j(x, y)$ can be derived from Eqs. (4) and (6), given by

$$\bar{w}_j(x, y) = \sum_{n=1}^N W_n(x, y) \tilde{q}_n^j. \quad (14)$$

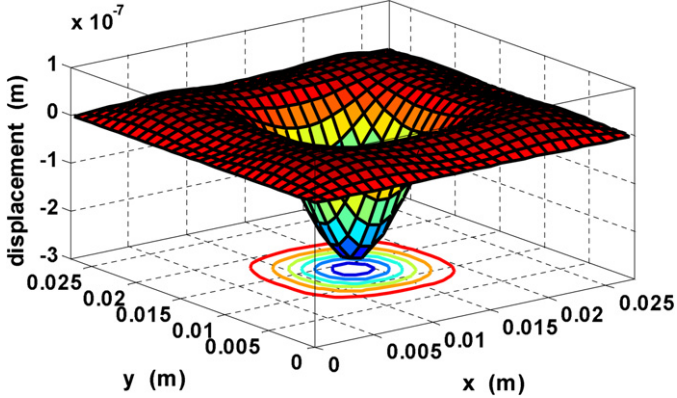
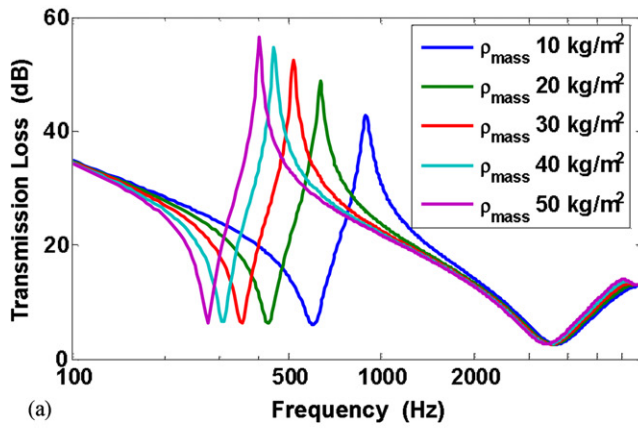
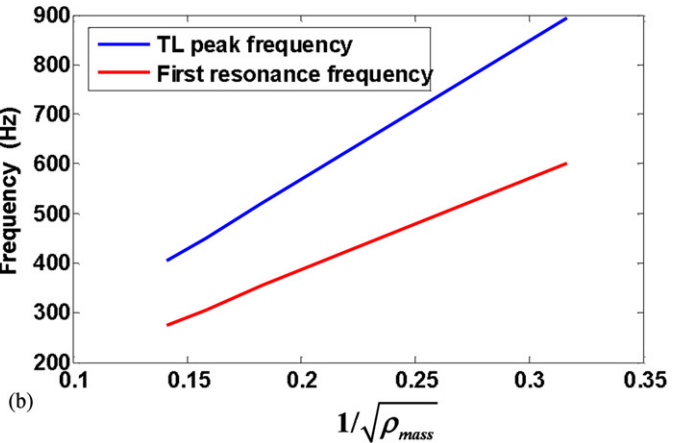


Fig. 3. The vibration mode of the membrane under the excitation of plane sound wave at TL peak frequency.

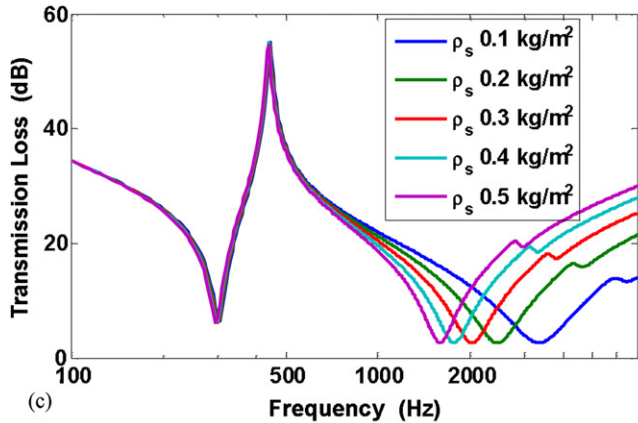
The first four eigenfrequencies are 338.68, 1540.1, 1540.1 and 2621.7 Hz, respectively, and the first and fourth eigenfrequencies are in very good agreement with the two valleys of the TL profile. To better understand the effects of the eigenmode on sound transmission behavior, the first four mode shapes of the membrane-type acoustic metamaterials were depicted in Fig. 2. For the first mode (Fig. 2(a)), the deformation is concentrated in the center, and it reduces rapidly away from the center, the whole membrane keeps in-phase at the first mode. At the second and third modes (Figs. 2(a), (b)), the deformations of the two half surfaces separated by the diagonal are the same amplitude but out-of-phase. For the fourth mode (Fig. 2(d)), the deformation is localized in the membrane while the mass at the center remains almost motionless. The average displacement of the membrane keep nonzero at the first and fourth modes, thus much sound power can be transmitted and TL valleys occur. While the average displacement of the whole surface equal to zero at the second and third modes, so these modes have no effect on the transmission of the sound. The first mode describes the locally resonant phenomenon (the mass and the adjacent membrane can be regard as a local resonator) of the membrane-mass structure, while the fourth mode is associated with the internal resonance of the elastic motion of the membrane. For the antiresonant mode of the local resonator, the vibration of the mass out-of-phase with the membrane, therefore the TL peak appears in the TL profile. The vibration mode of the membrane under the excitation of plane sound wave at TL peak frequency was depicted in Fig. 3. The displacement is mainly concentrated in the center, and the displacement near the mass out-of-phase with the other place of the membrane, averaged over



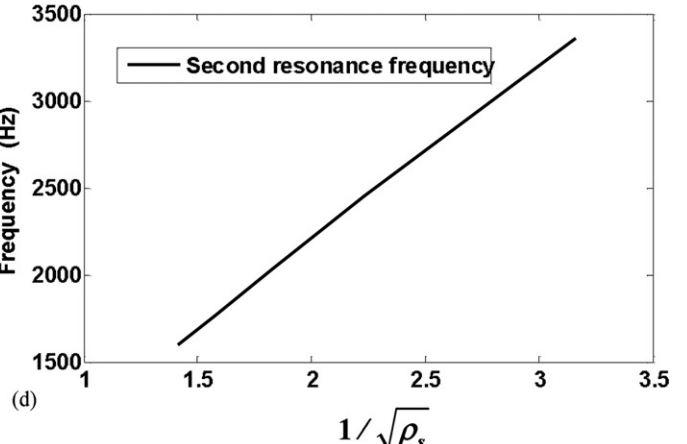
(a)



(b)



(c)



(d)

Fig. 4. The effects of mass and membrane surface density on transmission loss and characteristic frequencies. (a) The transmission loss with different mass surface density. (b) The relationship between mass surface density and first resonance and TL peak frequencies. (c) The transmission loss with different membrane surface density. (d) The relationship between mass surface density and second resonance frequencies.

我们可以得到膜型声学超材料的特征值方程

$$\{\omega \{[M] + [Q]\} - [K]\} \{\tilde{w}_q\} = 0. \quad (13)$$

特征值 ω 和特征向量 $\{\tilde{w}_q\}$ ($j = 1, \dots, N$) 可以使用雅可比方法获得。相应的自然模态形状 $\tilde{w}(x, y)$ 可以从方程 (4) 和 (6) 导出, 如下所示

$$\tilde{w}(x, y) = \sum_{n=1}^N W(x, y) \tilde{w}_q. \quad (14)$$

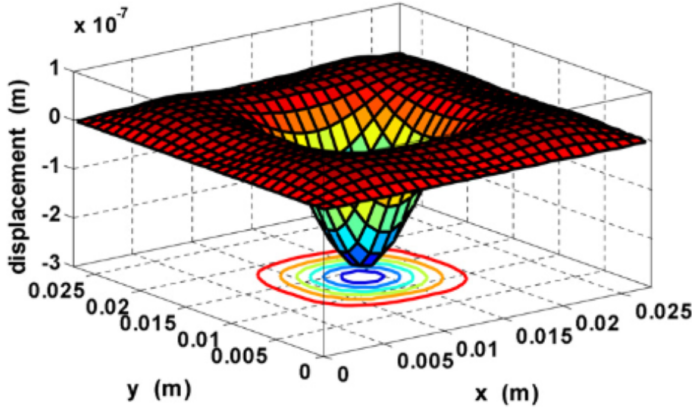
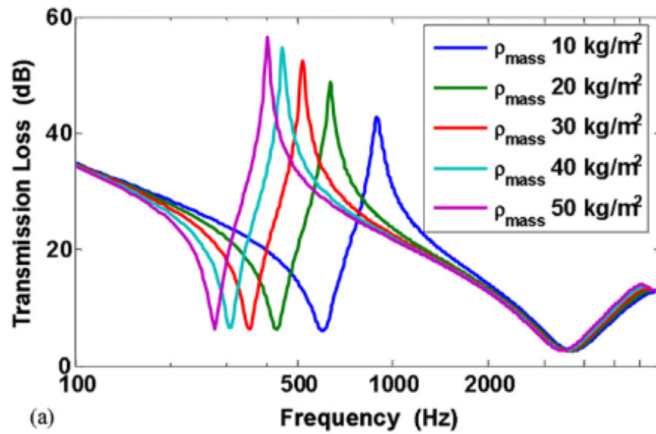
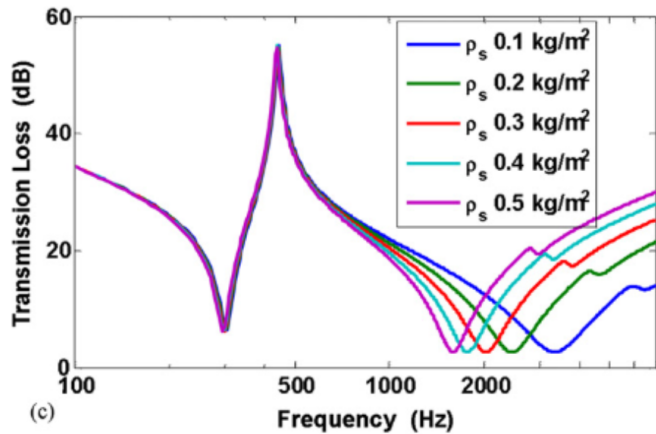


图 3. 在 TL 峰频率下平面声波激励下膜的振动模式。

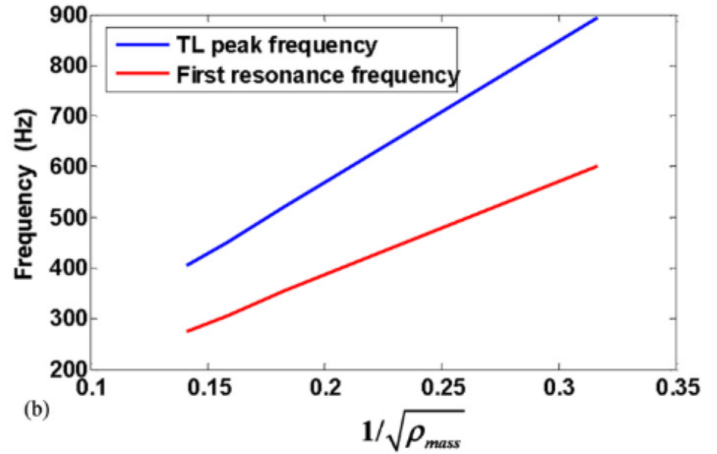
前四个特征频率分别为 338.68、1540.1、1540.1 和 2621.7 赫兹, 第一和第四特征频率与 TL 剖面的两个谷非常吻合。为了更好地理解特征模式对声传输行为的影响, 图 2 描述了膜型声学超材料的前四个模态形状。对于第一模态(图 2(a)), 变形集中在中心, 远离中心时迅速减小, 整个膜在第一模态下保持同相位。在第二和第三模态(图 2(a)、(b))中, 由对角线分隔的两个半表面的变形幅度相同但反相位。对于第四模态(图 2(d)), 变形局限在膜中, 而中心的质量几乎保持静止。膜的平均位移在第一和第四模态下保持非零, 因此可以传输大量声功率并产生 TL 谷。而整个表面的平均位移在第二和第三模态下等于零, 因此这些模态对声音的传输没有影响。第一种模式描述了膜-质量结构的局部谐振现象(质量和相邻膜可以被视为局部谐振器), 而第四种模式与膜的弹性运动的内部谐振有关。对于局部谐振器的抗谐振模式, 质量的振动与膜的振动反相, 因此在 TL 剖面中出现 TL 峰。在 TL 峰频率下, 膜在平面声波激励下的振动模式如图 3 所示。位移主要集中在中心, 质量附近的位移与膜的其他地方反相, 平均值超过



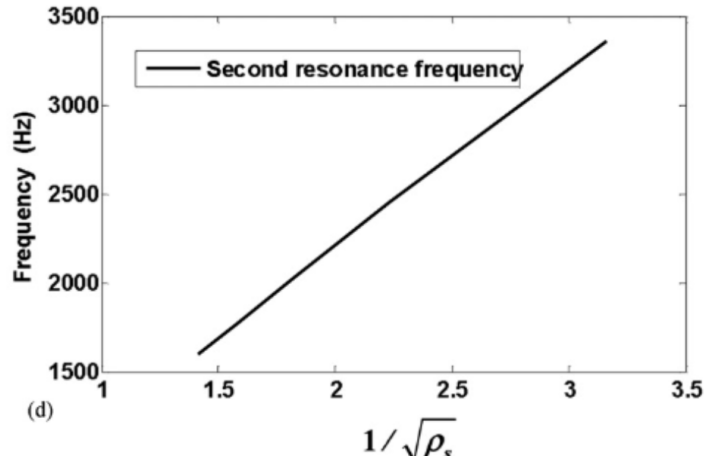
(a)



(c)



(b)



(d)

图 4. 质量和膜表面密度对传输损耗和特征频率的影响。 (a) 不同质量表面密度下的传输损耗。 (b) 质量表面密度与第一共振和 TL 峰频率之间的关系。 (c) 不同膜表面密度下的传输损耗。 (d) 质膜表面密度与第二共振频率之间的关系。

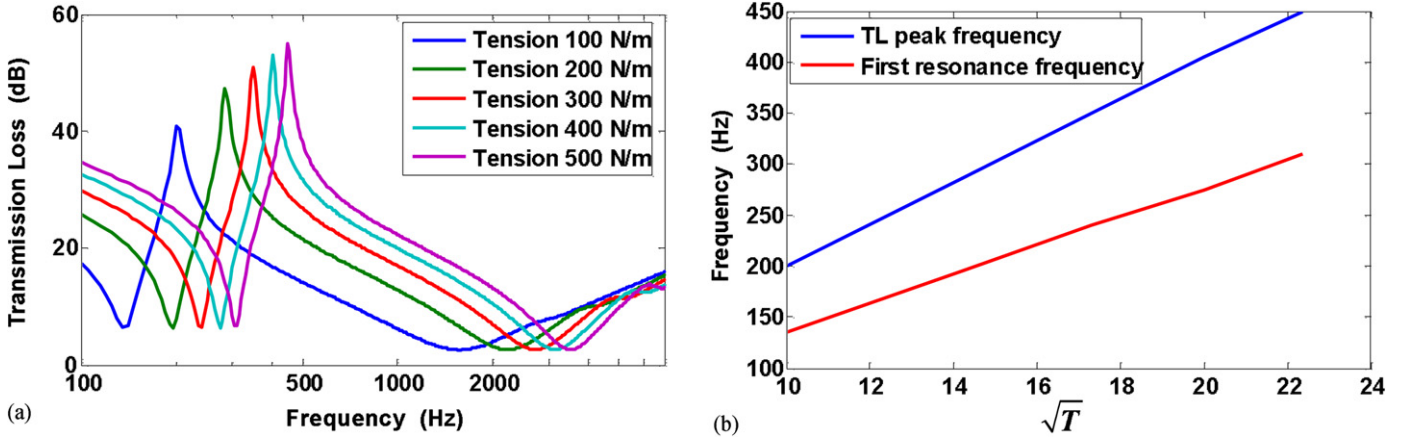


Fig. 5. The influence of membrane tensions on the TL profile and first resonance and TL peak frequencies. (a) The transmission loss with different membrane tension. (b) The relationship between membrane tension and first resonance and TL peak frequencies.

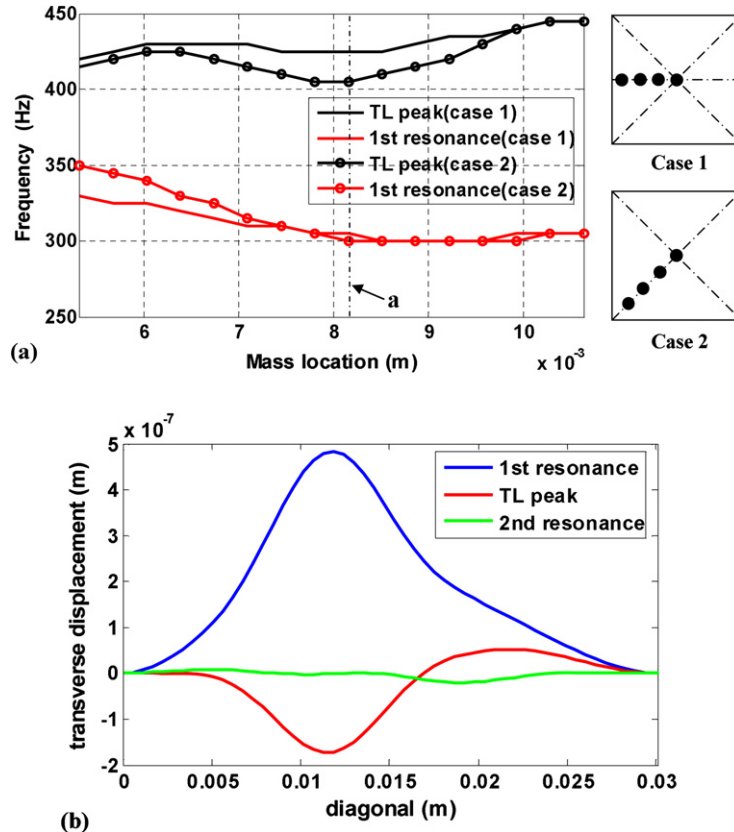


Fig. 6. The effects of mass position on the first resonance and TL peak frequencies and the transverse displacement of the membrane with mass glued at position a. (a) The variation of first resonance and TL peak frequencies with the mass position moving along the length (case 1) and the diagonal (case 2) of a square membrane. (b) The transverse displacement along the diagonal of the square membrane.

the entire membrane area, the positive and negative displacement amplitudes were counteracted.

The first TL valley and the TL peak, which are caused by the resonance and anti-resonance of the local resonator, will move following the parameters of the mass and tension. By contrast, the second TL valley, which is caused by the internal resonance of the membrane, is mainly determined by the parameters of the membrane and tension. The effects of mass and membrane surface density on transmission loss and characteristic frequencies were depicted in Fig. 4. Fig. 4(a) shows that the first resonance and TL peak frequencies move toward low-frequency as the mass surface density increasing, while the second resonance frequency has almost no change. The relationship between the mass surface den-

sity and the first resonance frequency, TL peak frequency is given by $f \propto 1/\sqrt{\rho_{\text{mass}}}$, which can be seen from Fig. 4(b). By contrary, increasing the membrane density, the second resonance frequency decreases accordingly, while first resonance and TL peak frequencies remain almost motionless (Fig. 4(c)). The second resonance frequency also inverse proportion with the square root of mass magnitude, which is given by $f \propto 1/\sqrt{\rho_s}$ (Fig. 4(d)). The influence of membrane tensions on the TL profile and first resonance and TL peak frequencies was shown in Fig. 5, the characteristic frequencies and the TL amplitude increase as the membrane tension increasing (Fig. 5(a)), that is reasonable, for larger tension cause the membrane more difficult to move, the relationship between them can be written as $f \propto \sqrt{T}$ (Fig. 5(b)).

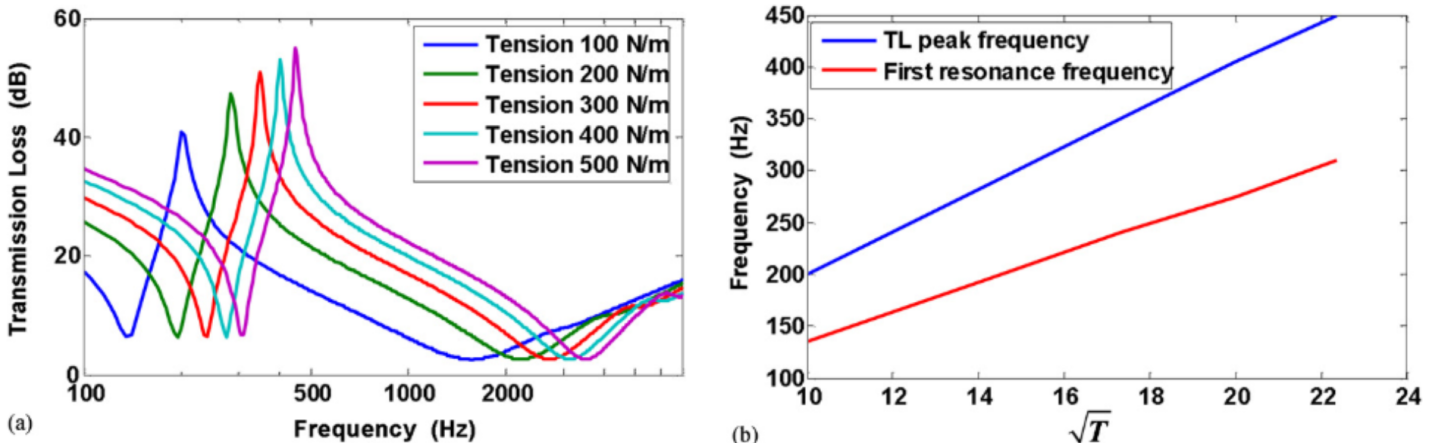


图 5. 膜张力对 TL 轮廓、第一共振和 TL 峰频率的影响。(a) 不同膜张力下的传输损耗。(b) 膜张力与第一共振和 TL 峰频率之间的关系。

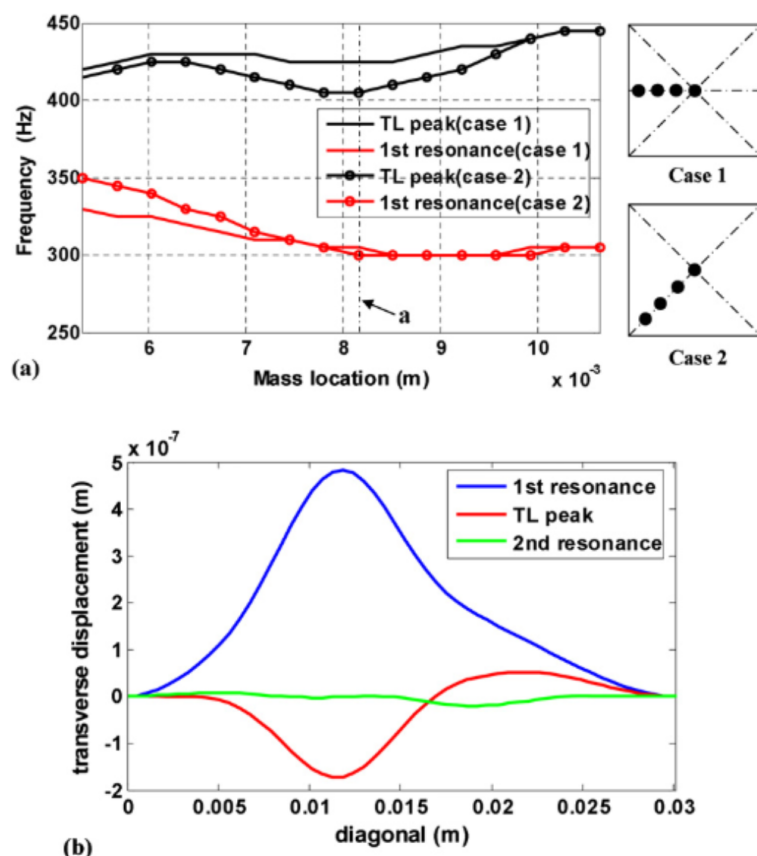


图 6. 质量位置对第一共振和 TL 峰频率以及带有质量粘在位置 a 的膜的横向位移的影响。(a) 质量位置沿着正方形膜的长度(案例 1)和对角线(案例 2)移动时第一共振和 TL 峰频率的变化。(b) 正方形膜对角线上的横向位移。

整个膜面积，正负位移幅度被抵消。

由于局部谐振器的谐振和反共振引起的第一个 TL 谷和 TL 峰将随着质量和张力的参数而移动。相反，由膜的内部谐振引起的第二个 TL 谷主要由膜和张力的参数决定。质量和膜表面密度对传输损耗和特征频率的影响在图 4 中描述。图 4(a)显示，随着质量表面密度的增加，第一个谐振和 TL 峰频率向低频移动，而第二个谐振频率几乎没有变化。

质量表面密度与第一共振频率、TL 峰频率之间的关系已给出

从图 4(b)可以看出，增加膜密度会导致第二共振频率相应下降，而第一共振和 TL 峰频率几乎保持不变(图 4(c))。第二共振频率也与质量大小的平方根成反比，即由 $f \propto 1/\sqrt{\rho}$

(图 4(d))。膜张力对 TL 轮廓、第一共振和 TL 峰频率的影响如图 5 所示，特征频率和 TL 幅度随着膜张力的增加而增加(图 5(a))，这是合理的，因为较大的张力使膜更难移动，它们之间的关系可以写成 $f \propto \sqrt{T}$ (图 5(b))。

The vibration modes should be changed once the location of the mass shift along the membrane, accordingly, the characteristic frequencies will be changed. Fig. 6(a) shows that the variation of first resonance and TL peak frequencies with the mass position moving along the length (case 1) and the diagonal (case 2) of a square membrane. At the position a, the first resonance frequency has almost no change, but the TL peak frequency reaches the smallest. The transverse displacement along the diagonal of the square membrane shows that the vibration displacement at the corner closest the mass in phase with the mass, while the corner fastest the mass out of phase with the vibration of the mass, that is different from the case of membrane with a central mass (Fig. 6(b)).

5. Conclusions

In this Letter we have developed an analytical approach to predict the sound transmission loss of membrane-type acoustic metamaterials. The validity of the analytical approach was confirmed by comparing the analytical results obtained in the present work with the FEA results reported in the existing publication. The analytical approach can be used to calculate the sound transmission loss of mass-loaded rectangular membrane; with a much smaller time and computational cost than the FEA. Eigenmode of the membrane unit (without load) was studied to find the physical explanation of the TL profile. The theoretical analysis and numerical results show that the properties of mass magnitude have more influence on the first TL valley frequency and peak frequency, while the second TL valley frequency depends strongly on the membrane property. The

effects of membrane tension and mass position on the TL and characteristic frequencies are also discussed.

Acknowledgements

This work was funded by the National Natural Science Foundation of China (Grant Nos. 11004249, 50905182, and 10902123).

References

- [1] Z. Liu, X. Zhang, Y. Mao, Y.Y. Zhu, Z. Yang, C.T. Chan, P. Sheng, *Science* 289 (2000) 1734.
- [2] Z. Liu, C.T. Chan, P. Sheng, A.L. Goertzen, J.H. Page, *Phys. Rev. B* 62 (2000) 2446.
- [3] Z. Liu, C.T. Chan, P. Sheng, *Phys. Rev. B* 71 (2005) 014103.
- [4] S. Hyeon, C. Mahn, Y. Mun, Z. Guo, C. Koo, *Phys. Lett. A* 373 (2009) 4464.
- [5] R. Zhu, G.L. Huang, H.H. Huang, C.T. Sun, *Phys. Lett. A* 375 (2011) 2863.
- [6] C.-I. Ding, X.-p. Zhao, *J. Phys. D, Appl. Phys.* 44 (2011) 215402.
- [7] K.M. Ho, C.K. Cheng, Z. Yang, X.X. Zhang, P. Sheng, *Appl. Phys. Lett.* 83 (2003) 5566.
- [8] H. Larabi, Y. Pennec, J.O. Vasseur, *Phys. Rev. E* 75 (2007) 066601.
- [9] M. Ambati, N. Fang, C. Sun, X. Zhang, *Phys. Rev. B* 75 (2007) 195447.
- [10] Z. Yang, J. Mei, M. Yang, N.H. Chan, P. Sheng, *Phys. Rev. Lett.* 101 (2008) 204301.
- [11] Z. Yang, H.M. Dai, N.H. Chan, G.C. Ma, P. Sheng, *Appl. Phys. Lett.* 96 (2010) 041906.
- [12] C.J. Naify, C.M. Chang, G. McKnight, S. Nutt, *J. Appl. Phys.* 108 (2010) 114905.
- [13] C.J. Naify, C.M. Chang, G. McKnight, F. Scheulen, S. Nutt, *J. Appl. Phys.* 109 (2011) 104902.
- [14] J.S. Wu, S.S. Luo, *J. Sound Vib.* 200 (1997) 179.
- [15] O. Kopmaz, S. Telli, *J. Sound Vib.* 251 (2002) 39.
- [16] K.T. Chan, X.Q. Wang, T.P. Leung, *J. Vib. Acoust.* 120 (1998) 944.
- [17] A.J. Mcmillan, A.J. Keane, *J. Sound Vib.* 192 (1996) 549.
- [18] F. Fahy, P. Gardonio, *Sound and Structural Vibration*, Academic Press, Oxford, 2008.

振动模式应该随着质量沿薄膜移动的位置而改变，相应地，特征频率也会改变。图 6(a)显示了质量位置沿着正方形薄膜长度（案例 1）和对角线（案例 2）移动时第一共振和 TL 峰频率的变化。在位置 a，第一共振频率几乎没有变化，但 TL 峰频率达到最小值。正方形薄膜对角线上的横向位移显示，靠近质量的角落的振动位移与质量同相位，而离质量最远的角落与质量的振动反相，这与带有中央质量的薄膜的情况不同（图 6(b)）。

5. 结论 在这封信中，我们开发了一种分析方法来预测膜型声学超材料的声音传输损失。通过将本工作中获得的分析结果与现有出版物中报道的有限元分析结果进行比较，验证了分析方法的有效性。这种分析方法可以用来计算负载矩形膜的声音传输损失；比有限元分析的时间和计算成本要小得多。研究了膜单元（无负载）的特征模式，以找到传输损失曲线的物理解释。理论分析和数值结果表明，质量大小对第一个传输损失谷频率和峰频率有更大影响，而第二个传输损失谷频率强烈依赖于膜的性质。

膜张力和质量位置对 TL 和特征频率的影响也在讨论中。

致谢

这项工作得到了中国国家自然科学基金的资助（项目编号 11004249、50905182 和 10902123）。

参考资料

- [1] 刘志, 张旭, 毛洋, 朱亚亚, 杨忠, 陈才铁, 盛平, 科学 289 (2000) 1734.
- [2] 刘忠, 陈才铁, 盛平, A.L. Goertzen, J.H. Page, Phys. Rev. B 62 (2000) 2446.
- [3] 刘忠, 陈才铁, 盛平, 物理评论 B 71 (2005) 014103.
- [4] S. Hyeon, C. Mahn, Y. Mun, Z. Guo, C. Koo, Phys. Lett. A 373 (2009) 4464.
- [5] R. 朱, G.L. 黄, H.H. 黄, C.T. 孙, Phys. Lett. A 375 (2011) 2863.
- [6] 丁昌利, 赵晓平, J. Phys. D, Appl. Phys. 44 (2011) 215402. [7] K.M. Ho, C.K. Cheng, Z. Yang, X.X. Zhang, P. Sheng, Appl. Phys. Lett. 83 (2003) 5566.
- H. Larabi, Y. Pennec, J.O. Vasseur, Phys. Rev. E 75 (2007) 066601.
- M. Ambati, N. Fang, C. Sun, X. Zhang, Phys. Rev. B 75 (2007) 195447.
- [10] Z. 杨, J. 梅, M. 杨, N.H. 陈, P. 盛, Phys. Rev. Lett. 101 (2008) 204301. [11] Z. 杨, H.M. 戴, N.H. 陈, G.C. 马, P. 盛, Appl. Phys. Lett. 96 (2010) 041906.
- [12] C.J. Naify, C.M. Chang, G. McKnight, S. Nutt, J. Appl. Phys. 108 (2010) 114905. [13] C.J. Naify, C.M. Chang, G. McKnight, F. Scheulen, S. Nutt, J. Appl. Phys. 109 (2011) 104902.
- J.S. Wu, S.S. Luo, J. Sound Vib. 200 (1997) 179.
- O. Kopmaz, S. Tellis, J. Sound Vib. 251 (2002) 39.
- [16] K.T. Chan, X.Q. Wang, T.P. Leung, J. Vib. Acoust. 120 (1998) 944.
- A.J. McMillan, A.J. Keane, J. Sound Vib. 192 (1996) 549.
- F. Fahy, P. Gardonio, 声音和结构振动, 学术出版社, 牛津, 2008.